Biological Trace Element Research
https://doi.org/10.1007/s12011-022-03107-8

Copper Oxide Nanoparticles Exhibit Cell Death Through Oxidative Stress Responses in Human Airway Epithelial Cells: a Mechanistic Study

Nida N. Farshori[1] · Maqsood A. Siddiqui[2] · Mai M. Al-Oqail[1] · Ebtesam S. Al-Sheddi[1] · Shaza M. Al-Massarani[1] · Maqusood Ahamed[3] · Javed Ahmad[2] · Abdulaziz A. Al-Khedhairy[2]

Received: 16 December 2021 / Accepted: 4 January 2022

Abstract

Copper oxide nanoparticles (CuONPs) are purposefully used to inhibit the growth of bacteria, algae, and fungi. Several studies on the beneficial and harmful effects of CuONPs have been conducted in vivo and in vitro, but there are a few studies that explain the toxicity of CuONPs in human airway epithelial cells (HEp-2). As a result, the purpose of this study is to look into the dose-dependent toxicity of CuONPs in HEp-2 cells. After 24 h of exposure to 1–40 µg/ml CuONPs, the MTT and neutral red assays were used to test for cytotoxicity. To determine the mechanism(s) of cytotoxicity in HEp-2 cells, additional oxidative stress assays (LPO and GSH), the amount of ROS produced, the loss of MMP, caspase enzyme activities, and apoptosis-related genes were performed using qRT-PCR. CuONPs exhibited dose-dependent cytotoxicity in HEp-2 cells, with an IC_{50} value of ~ 10 µg/ml. The morphology of HEp-2 cells was also altered in a dose-dependent manner. The involvement of oxidative stress in CuONP-induced cytotoxicity was demonstrated by increased LPO levels and ROS generation, as well as decreased levels of GSH and MMP. Furthermore, activated caspase enzymes and altered apoptotic genes support CuONPs' ability to induce apoptosis in HEp-2 cells. Overall, this study demonstrated that CuONPs can cause apoptosis in HEp-2 cells via oxidative stress; therefore, CuONPs may pose a risk to human health and should be handled and used with caution.

Keywords Copper oxide nanoparticles · HEp-2 cells · Cytotoxicity · Oxidative stress · Caspase activity · Gene expression

Introduction

Copper oxide nanoparticles (CuONPs) are widely used in a variety of consumer products, including electronics, cosmetics, sensors, textiles, paints, and timber protection [1]. CuONPs are also used in a variety of other products, including intrauterine contraceptive devices, heat transfer fluids, semiconductors, and electronic chips [2]. Furthermore, CuONPs have been used as antifungal agents in plastics, coatings, and textiles [3]. CuONPs, due to their electrochemical properties, are suitable for use in graphite surface coating to improve capacitance properties [4]. The enormous growth in consumption and manufacturing has raised major concerns about the negative effects on human health and the environment [5]. A large number of studies have shown that it is harmful to organisms and cells [6]. CuONPs have been reported to be effective against a wide variety of microorganisms [7]. CuONPs have also been shown to be toxic to zebrafish [8], crustaceans [9], microalgae [10], bacteria [11], and yeast [12]. CuONPs have previously been shown in vitro to cause cytotoxicity, genotoxicity, mitochondrial dysfunction, oxidative stress, and apoptosis [13, 14]. CuONP-induced cell death has also been documented in human cell lines, such as liver HepG2 [15], lung epithelial A549 [16], cardiac vascular HCMECs [17], kidney HEK293 [18], neuronal SHSY5Y, H4 [19], skin epidermal HaCaT [20], and endothelial HUVECs [21]. Recently, studies on cell lines

✉ Maqsood A. Siddiqui
maqsoodahmads@gmail.com; masiddiqui@ksu.edu.sa

[1] Department of Pharmacognosy, College of Pharmacy, King Saud University, Riyadh 11495, Saudi Arabia

[2] DNA Research Chair, Zoology Department, College of Science, King Saud University, P.O. Box 2455, Riyadh 11451, Saudi Arabia

[3] King Abdullah Institute for Nanotechnology, King Saud University, Riyadh 11451, Saudi Arabia

Published online: 08 January 2022

(in vitro) and rat models (in vivo) revealed that the toxicity of CuONPs is associated with elevated levels of ROS, oxidative stress, and antioxidants depletion [14, 22]. These free radicals and oxidative stress trigger a series of cellular events, including apoptosis [14]. A number of studies have found that CuONPs can be genotoxic depending on their size, shape, concentration, and exposure time [23]. These reports clearly state that additional research is required to assess the toxic responses of CuONPs and their toxicity mechanisms in order to assess the potential risk to human health. The presence of NPs in the environment is significant in terms of their impact on human health. Because of their small size and large surface area, these nanoparticles can easily enter the body through the airway and cause harm to epithelial tissues. As a result, they can cross the cell membrane with ease, causing cell disruption and translocation between cells [6]. Because of the high impact usage of CuONPs, it is critical to disapprovingly evaluate the toxicity of CuONPs. Nonetheless, there is a paucity of data on the potentially harmful effects of CuONP exposure in humans. As a result, in this study, we used human airway epithelial cells (HEp-2) to investigate the cytotoxic responses of CuONPs in vitro. Furthermore, the mechanisms or pathways involved in CuONP-induced cytotoxicity were investigated.

Materials and Methods

Materials

CuONPs (from Sigma-Aldrich of < 50 nm particle size) were used in this study. The stock concentration of CuONPs (10 mg/ml) was freshly prepared in Milli-Q water and sonicated before use in the study.

Characterization of CuONPs

X-ray Diffraction (XRD)

The crystalline nature of CuONPs was achieved by XRD pattern. The XRD pattern of CuONPs was developed by using a PANalytical X'Pert X-ray diffractometer equipped with a Ni filter by Cu K_α ($\lambda = 1.54056$ Å) radiations as X-ray source.

Transmission Electron Microscopy

Shape and size of CuONPs were measured by transmission electron microscopy (JEM-2100F, JEOL Inc., Japan) at an accelerating voltage of 200 kV. CuONPs were suspended in deionized water at a concentration of 1 mg/ml and sonicated at 40 W for 15 min at room temperature (RT). The stock solution was then diluted to a working solution concentration of 50–100 µg/ml. A drop of CuONP suspension was then placed onto a copper grid, air-dried, and examined under FETEM.

Dynamic Light Scattering

The zeta potential and hydrodynamic size of CuONPs in culture medium and water were determined using dynamic light scattering (DLS) according to the method of Murdock et al. [24]. CuONPs were suspended in culture medium and water. Following the sonication, DLS study was performed at room temperature.

Cell Culture

Human airway epithelial cells (HEp-2, ATCC; CCL-23™) were obtained from the American Type Culture Collection (ATCC, Manassas, VA, USA) and used in this study between passage numbers 20 and 25. The HEp-2 cells were grown in DMEM supplemented with 10% FBS, streptomycin, and penicillin. HEp-2 cells were maintained in a cell culture incubator at 37 °C in a humidified atmosphere with 5% CO_2.

CuONPs Treatment

Using 10 mg/ml of CuONP stock solution, a range of concentrations (1, 2, 5, 10, 20, and 40 µg/ml) were prepared in culture medium for the treatment of cells for 24 h.

Cytotoxicity of CuONP-Treated HEp-2 Cells by MTT Assay

HEp-2 cells were plated into a 96-well plate and grown overnight. The medium was then aspirated and replaced with a medium containing 1, 2, 5, 10, 20, and 40 µg/ml of CuONPs. After 24-h incubation, 10 µl of MTT solution (5 mg/ml stock) was added in wells. The solution was washed out after 4 h of incubation at 37 °C, and 200 µl DMSO was added to each well. After gentle mixing, the developed purple color was measured at 550 nm [25].

Cytotoxicity of CuONP-Treated HEp-2 Cells by NRU Assay

In a 96-well culture plate, HEp-2 cells were exposed to CuONPs for 24 h at 1, 2, 5, 10, 20, and 40 µg/ml. Following incubation, the existing medium was aspirated and replaced with NR-containing medium (50 µg/ml), which was then incubated at 37 °C for 3 h. After washing the wells with washing solution, the dye was extracted in a solution of 50% ethanol, 49% water, and 1% acetic acid. After gentle mixing, an absorbance reading was recorded at 550 nm wavelength [26].

% cell viability was determined using the following formula:

$$\%\ \text{cell viability} = \frac{\text{mean absorbance of treated group}}{\text{mean absorbance of control group}} \times 100$$

Morphological Alterations

HEp-2 cells were grown in a 96-well plate at a density of 1×10^4 cells. The old medium was then replaced with medium containing various concentrations (1, 2, 5, 10, 20, and 40 µg/ml). After 24 h of treatment, morphological changes were observed under a microscope (Olympus CKX41, Japan) equipped with a live camera at a magnification of 20×.

Lipid Peroxidation (LPO) Measurement

LPO was quantified using the TBA reagent according to the protocol defined by Buege and Aust [27]. In brief, HEp-2 cells were exposed for 24 h to CuONPs at concentrations of 10, 20, and 40 µg/ml. After exposure, 1 ml cellular extract and 2 ml TBA reagent were mixed and heated at 100 °C for 20 min. After cooling the mixture to room temperature, the absorbance was measured spectrophotometrically at 535 nm.

Glutathione (GSH) Measurement

GSH was measured using the protocol of Chandra et al. [28]. HEp-2 cells were exposed to 10, 20, and 40 µg/ml of CuONPs for 24 h. The cells were then centrifuged, resuspended in 10% TCA, and sonicated. After centrifugation, 1 ml of supernatant was added to 2 ml of DTNB mixture (10 mM DTNB, 20 mM EDTA, and 400 mM Tris buffer pH = 8.9). The absorbance at 420 nm was measured after 10 min of incubation at 37 °C.

ROS Measurement

HEp-2 cells were seeded in 24-well plates and grown at 37 °C overnight. The medium was then aspirated and replaced with a medium containing 10, 20, and 40 µg/ml of CuONPs. After 24-h incubation, the cells were washed and incubated with 20 µM of DCFDA dye for 60 min. The live imaging of the cells was done under a fluorescence microscope (Olympus) equipped with a camera. DCF intensity was also measured in the cells at 485 nm and 538 nm emission and excitation, respectively [29].

MMP

MMP was performed following the protocol of Al-Oqail et al. [30], using rhodamine-123 (Rh-123) fluorescence staining. After 24 h of exposure to CuONPs at 10, 20, and 40 µg/ml, the HEp-2 cells were washed and incubated with Rh-123 (10 µM) for 30 min at 37 °C. The fluorescence of mitochondrial transmembrane potential was then examined by capturing images with a fluorescence microscope and measuring the fluorescence at excitation and emission at 485 and 538 nm, respectively, with a fluorescence microplate reader (Fluoroskan Ascent, Thermo-Scientific, Finland). The values of MMP obtained in control were considered 100%.

Caspase-3 and Caspase-9 Enzyme Activities

To further assess the effect of CuONPs on cell apoptosis, the enzymatic activity of caspase-3 and caspase-9 was done by commercially available kits. After 24 h of CuONPs exposure, cultured HEp-2 cells were collected, and experiments were carried out according to the protocol provided with the assay kits (BioVision, USA). The samples were measured using a microplate spectrophotometer, and the values of caspase-3 and caspase-9 activity obtained were presented as a fold change compared to the control.

Gene Expression by qRT-PCR

HEp-2 cells were exposed to 40 µg/ml of CuONPs for 24 h, and total RNA was extracted using RNeasy mini kit (Qiagen, Germany). The total RNA was quantified using a spectrophotometer (Nanodrop 8000). Then, 1 µg RNA was reverse-transcribed into cDNA using reverse transcriptase kit. cDNA was used as a template for real-time quantitative PCR using SYBR Master Mix to quantify gene transcription. Our previous publications described the primers and detail protocol [31, 32].

Statistical Analysis

All the results are presented as mean ± SD. The data were examined by one-way analysis of variance with post hoc Dunnett's test for comparison. A difference of $p < 0.05$ was considered statistically significant.

Results

Characterization of CuONPs

XRD pattern of CuONPs evidently displays the crystalline nature of the material (Fig. 1a). Using Scherrer's equation [33], the crystallite size was assessed from the XRD pattern. The average crystallite size of the CuONPs as determined from XRD was ~ 38 nm.

The average size of the CuONPs determined from TEM image was ~ 37 nm, which supports the XRD results. The TEM images, as shown in Fig. 1b, revealed that the majority

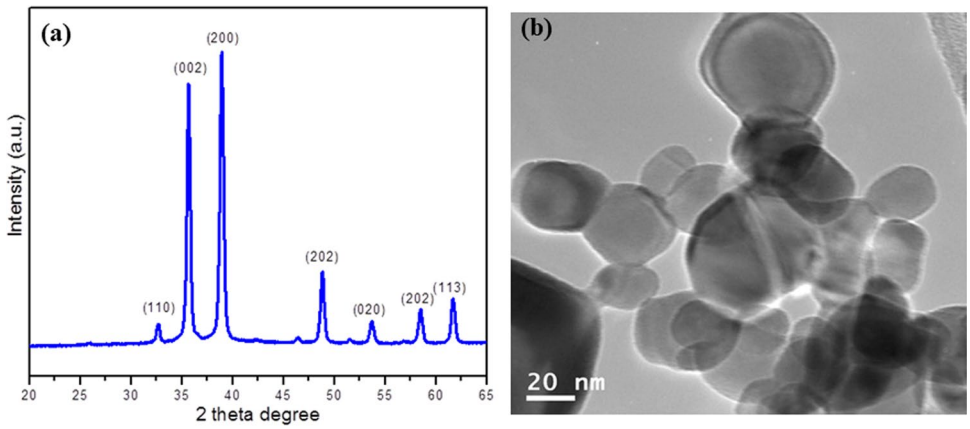

Fig. 1 Characterization of copper oxide nanoparticles (CuONPs): **a** X-ray powder diffraction pattern of CuONPs and **b** transmission electron microscopic image of CuONPs at 20 nm

Table 1 Characterization of CuONPs in H_2O and culture medium

Dispersant	Hydrodynamic size (nm)	Zeta potential (mV)
Water (H_2O)	275 ± 27	− 11 ± 2.6
Culture medium	243 ± 43	− 14 ± 3.3

of the NPs were spherical in shape with smooth surfaces. The size was determined by measuring over 75 NPs in a random field of view. The physiochemical characteristics of the CuONPs are provided in Table 1. The normal hydrodynamic size of CuONPs in H_2O and culture medium as determined by dynamic light scattering was about 275 ± 27 nm and 243 ± 43 nm, respectively. The zeta potential of CuONPs in H_2O and culture medium was about − 11 mV and − 14 mV, respectively.

Cytotoxicity of CuONPs

CuONP-induced cytotoxicity in HEp-2 cells was evaluated by MTT and NRU assays (Fig. 2a, b). CuONPs reduced the viability of HEp-2 cells in a dose-dependent manner, according to the findings. The viability of HEp-2 cells was found as 29%, 36%, 48%, 72%, and 88% by the MTT assay (Fig. 2a) and 33%, 39%, 52%, 75%, and 92% by the NRU assay (Fig. 2b) at 40, 20, 10, 5, and 2 µg/ml, respectively. The IC_{50} values of CuONPs in HEp-2 cells were 9.6 µg/ml and 10.4 µg/ml, respectively, according to the MTT and NRU assays.

Cell Morphology

The HEp-2 cells were treated with CuONPs for 24 h and observed under an optical microscope. The control cells have a regular shape and no membrane damage, as shown in Fig. 2c. Cells exposed to a 5 µg/ml concentration of CuONPs, on the other hand, began to leave the surface and become rounded. With increasing doses of CuONPs, the HEp-2 cells began to lose their cellular contents, resulting in cell death after 24-h exposure.

Oxidative Damage

The potential of CuONP-induced oxidative damage was assessed in HEp-2 cells at 10, 20, and 40 µg/ml by measuring the LPO and GSH levels, which are commonly used endpoints to quantify oxidative damage in cells. CuONP exposure increased the level of LPO by 134%, 162%, and 197% at 10, 20, and 40 µg/ml, respectively (Fig. 3a). GSH level, on the other hand, was decreased by 29%, 48%, and 66% at 10, 20, and 40 µg/ml of CuONPs, respectively (Fig. 3b). Changes in oxidative stress markers (LPO and GSH) in HEp-2 cells were concentration-dependent and statistically significant when compared to control (**$p < 0.01$).

ROS Generation

The ROS generation induced by CuONPs in HEp-2 cells was evaluated at 10, 20, and 40 µg/ml concentrations (Fig. 4a, b). Fluorescence microscopic images revealed that HEp-2 cells treated with CuONPs exhibited a dose-dependent intensity of DCF in terms of green fluorescence with high intensity at 40 µg/ml when compared to the untreated control (Fig. 4a). CuONPs inhibited ROS generation in HEp-2 cells by 123%, 175%, and 218% at 10, 20, and 40 µg/ml concentrations for 24 h when compared to the control (Fig. 4b).

MMP Level

To evaluate the impact of CuONPs on mitochondria and its mechanism of action, the effects of CuONPs on HEp-2 cells were assessed by using Rh-123 fluorescence staining. When compared to an untreated control, CuONPs had a significant effect on mitochondrial membrane potential. As shown in Fig. 5a, the red fluorescence images of Rh-123 in HEp-2

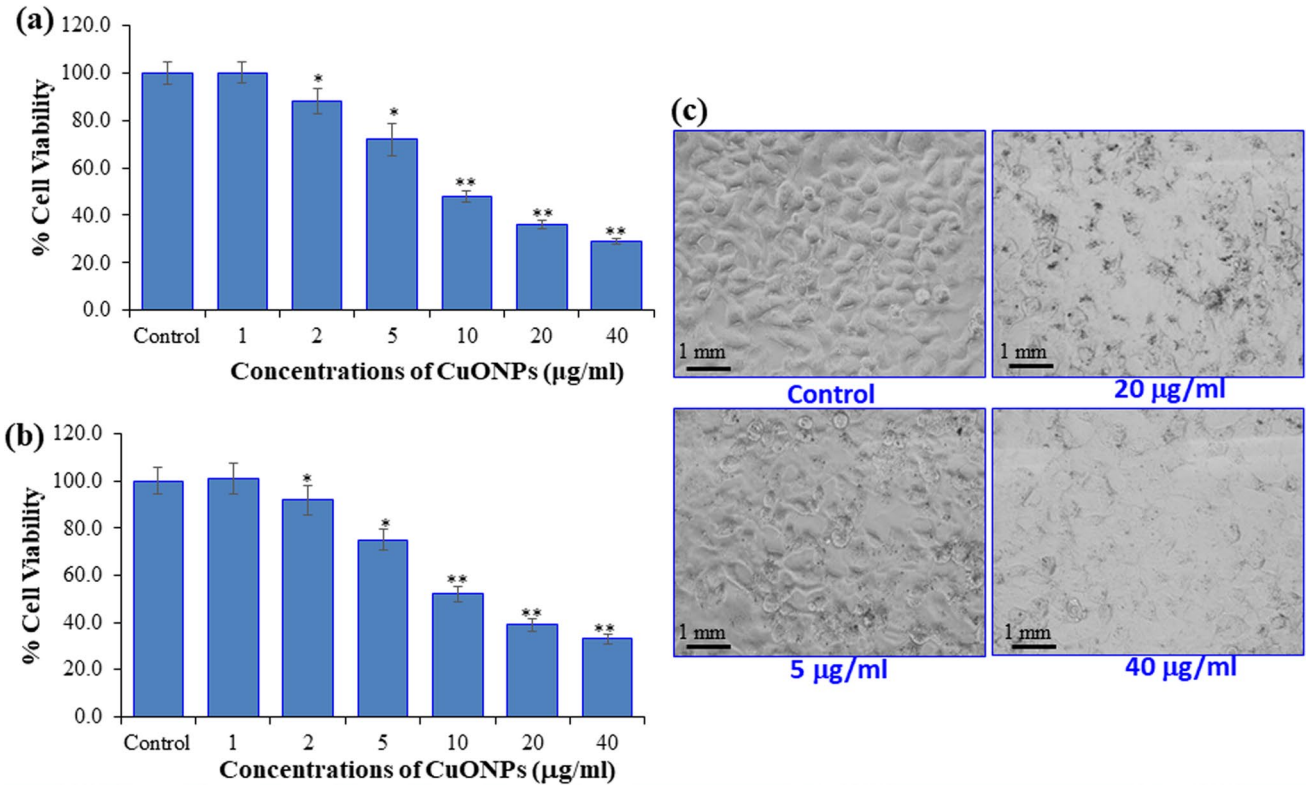

Fig. 2 Cytotoxicity assessments by **a** MTT assay and **b** neutral red uptake (NRU) assay, and **c** representative images of morphological alterations in human airway epithelial (HEp-2) cell line. HEp-2 cells were exposed to CuONPs at 1–40 µg/ml for 24 h. Images were taken using an inverted phase contrast microscope (Olympus CKX41, Japan) at 20× magnification. Values are mean ± SD of three independent experiments. *$p < 0.05$, ** $p < 0.01$ vs control. Scale bar = 1 mm

cells exposed to CuONPs showed a dose-dependent decrease when compared to the control. At 10, 20, and 40 µg/ml concentrations of CuONPs, the intensity of Rh-123 fluorescence was reduced by 15%, 39%, and 58%, respectively (Fig. 5b).

Caspase Enzyme Activity

Caspase-3 and caspase-9 activities were evaluated as markers of apoptosis initiation. CuONPs activated the caspase-3 and caspase-9 enzymes in a concentration-dependent manner, as shown in Fig. 6. In HEp-2 cells exposed to CuONPs for 24 h, caspase-3 was activated up to 1.6-, 2.1-, and 3.2-fold, and caspase-9 was activated up to 1.8-, 2.4-, and 3.8-fold, respectively.

Apoptosis Assay

Quantitative real-time PCR was used to quantify the mRNA level of apoptosis genes (p53, bax, bcl2, caspases 3 and 9) in HEp-2 cells treated with CuONPs at a concentration of 40 µg/ml for 24 h. The study's findings revealed that CuONP exposure significantly altered the mRNA levels of apoptosis genes (Fig. 7). The mRNA level of p53 gene was 2.9-fold higher in treated cells when compared to control. Furthermore, the expression of caspase 3 and 9 genes was 2.7- and 3.2-fold, respectively, higher in treated HEp-2 cells. The mRNA expression of proapoptotic gene bax was 2.7-fold higher and antiapoptotic gene bcl2 was 1.45-fold lower when compared to control (Fig. 7).

Discussion

CuONPs have been extensively used in a variety of products [34]. Because of their small size and large surface area, these nanoparticles can easily enter the body through the airway and cause harm to epithelial tissues. As a result, it is critical to understand the molecular mechanism underlying CuONP-induced epithelial dysfunction. As a result, the toxic responses of CuONPs in human airway epithelial cells (HEp-2) were evaluated in the current study. CuONPs significantly induced cytotoxicity in HEp-2 cells, according to the findings. MTT and NRU assays revealed that CuONPs cause HEp-2 cell death in a dose-dependent manner at concentrations ranging from 2 to 40 µg/ml. Several reports have indicated that CuONPs can cause toxicity in cultured cells

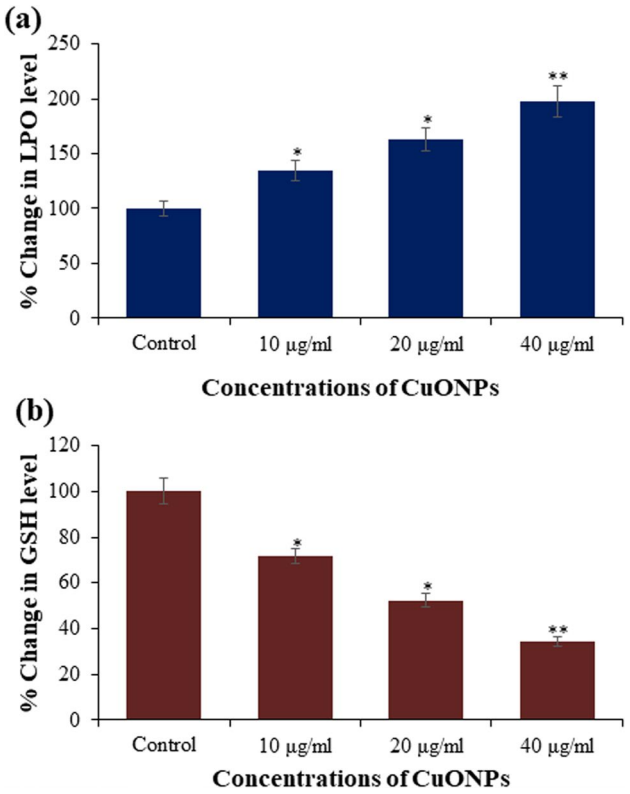

Fig. 3 Copper oxide nanoparticles (CuONPs) induced oxidative stress in human airway epithelial cells (HEp-2). The cells were exposed to CuONPs at 10–40 µg/ml for 24 h. **a** Lipid peroxidation and **b** glutathione depletion. $*p < 0.05$, $**p < 0.01$ vs control

in a dose-dependent manner. These findings are consistent with previous research that found CuONPs induced dose-dependent cytotoxicity in human endothelial cells HUVEC (10–40 µg/ml for 24 h) [21], liver cells HepG2 (2–50 µg/ml for 24 h) [14], lung epithelial cells A-549 (5–15 µg/ml for 24 h) [35], and human embryonic kidney cells HEK293 (3–300 µg/ml for 48 h) [18]. The IC_{50} values of CuONPs were found to be 9.6 µg/ml and 10.4 µg/ml by MTT and NRU assays, respectively, at 24-h exposure. Similarly, Fu [15] found significant cytotoxicity of CuONPs in this concentration range in human liver cells HepG2 with an IC_{50} value of 8 µg/ml.

One of the mechanisms of cytotoxicity persuaded by nanoparticles is the involvement of oxidative stress [36]. According to current research, CuONP-induced oxidative stress was measured by an increased in LPO and decreased in GSH levels [18]. In this study, CuONP-induced oxidative damage was also observed in this study, with an increase of 134%, 162%, and 197% in LPO level and a decrease of 29%, 48%, and 66% in GSH level at 10, 20, and 40 µg/ml, respectively, after 24-h exposure. These findings showed that when CuONPs were exposed to HEp-2 cells, they produced a dose-dependent increase in LPO and a decrease in GSH levels, indicating that oxidative stress played a role in HEp-2 cytotoxicity. There are numerous reports that back up our findings. CuONPs have been shown in studies to be toxic to human cells via oxidative stress [16, 37]. Previous research suggested that excessive ROS production is a major cause of cytotoxicity after NP exposure [38]. ROS is produced in physiological condition as a natural response to the regular metabolism of oxygen and plays an important role in several cellular signaling pathways [39]. However, following the

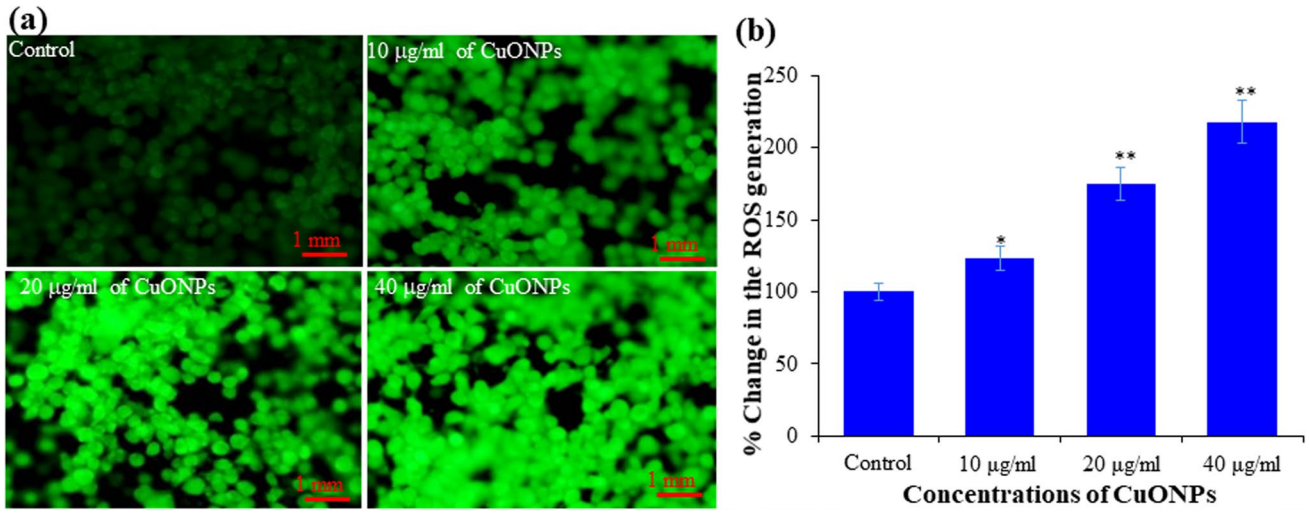

Fig. 4 Copper oxide nanoparticles (CuONPs) induced ROS generation in human airway epithelial cells (HEp-2). **a** Representative fluorescence images showing ROS generation in HEp-2 cells after the exposure of CuONPs at 10, 20, and 40 µg/ml for 24 h. **b** Percentage change in ROS generation in HEp-2 cells after the exposure of CuONPs at 10, 20, and 40 µg/ml for 24 h. $*p < 0.05$, $**p < 0.01$ vs control. Scale bar = 1 mm

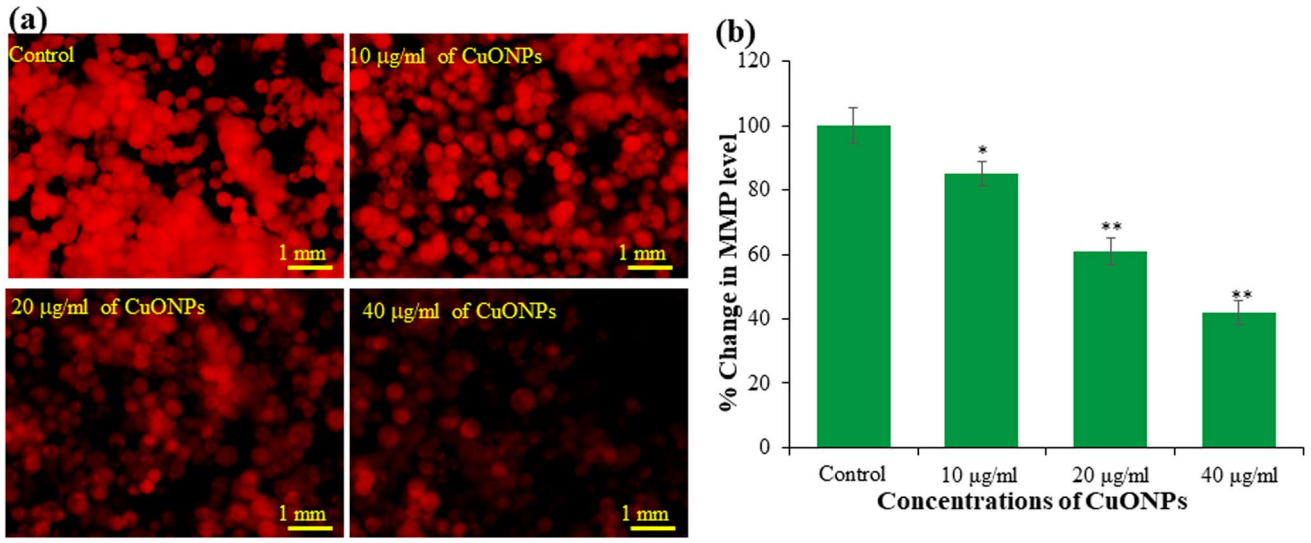

Fig. 5 Copper oxide nanoparticles (CuONPs) induced MMP loss in human airway epithelial cells (HEp-2). **a** Representative fluorescence images showing MMP loss in HEp-2 cells after the exposure of CuONPs at 10, 20, and 40 µg/ml for 24 h. **b** Percentage change in loss of MMP in HEp-2 cells after the exposure of CuONPs at 10, 20, and 40 µg/ml for 24 h. $*p<0.05$, $**p<0.01$ vs control. Scale bar = 1 mm

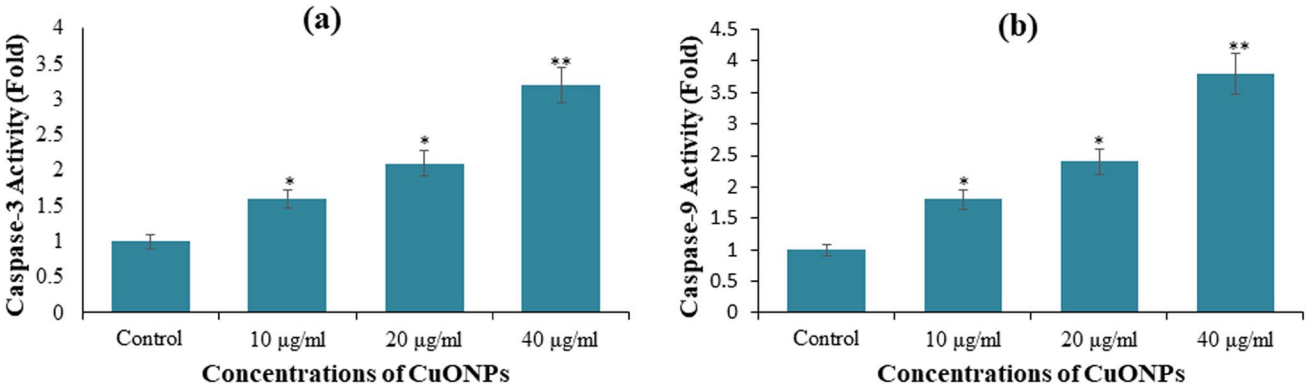

Fig. 6 Copper oxide nanoparticles (CuONPs) induced apoptotic responses in human airway epithelial cells (HEp-2). **a** Caspase-3 enzyme activity and **b** caspase-9 enzyme activity in HEp-2 cells after the exposure of CuONPs at 10, 20, and 40 µg/ml for 24 h. $*p<0.05$, $**p<0.01$ vs control

exposure of CuONPs, the ROS generation was significantly increased in HEp-2 cells. These results were supported by other published reports exhibiting CuONP-induced cell death through overproduction of ROS in cultured cells [40]. The most common mechanistic explanations for ROS are that metal ions released by CuONPs promote ROS production by interfering with mitochondrial respiration [41]. CuONPs have previously been shown to reduce mitochondrial membrane potential, potentially leading to cell death [37]. Despite considerable methodical development, mitochondria remain a potential target of nanoparticles [42]. Furthermore, mitochondria act as a key modulator in the cell signaling cascade involved in programmed cell death [43]. There are a number of fluorescence probe available to measure mitochondrial membrane potential (MMP). Herein, the effects of CuONPs were measured by Rh-123 staining. Rh-123 is a cationic dye that displays dependent localization in mitochondria with intracellular fluorescence [44]. As shown in Fig. 5, exposure to CuONPs reduced MMP in HEp-2 cells in a concentration-dependent manner when compared to unexposed control cells. As a result, CuONPs may penetrate the membrane and activate intracellular signaling pathways, resulting in ROS and apoptosis, as previously reported with CuONP exposure [37].

Caspase-3 and caspase-9 enzyme activity was examined to confirm the CuONP-induced apoptosis in HEp-2 cells. Caspase families play an important role in the regulation of cell death signaling transduction in mammals. Proapoptotic

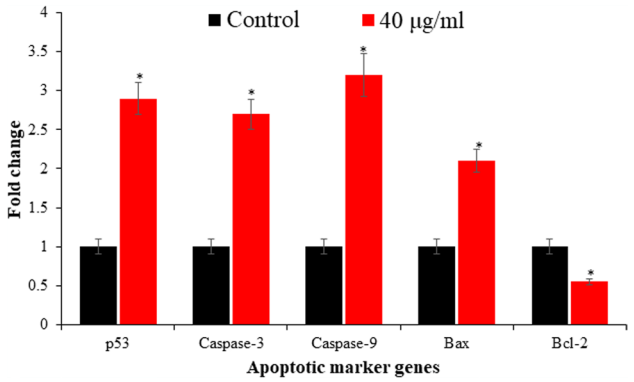

Fig. 7 The mRNA expression of apoptotic marker genes in HEp-2 cells after the exposure of CuONPs at 40 µg/ml for 24 h. The mRNA expression of genes was assessed by using quantitative real-time PCR (qRT-PCR). *$p < 0.05$ vs control

caspases, in particular, play a dynamic role in this regulation [45]. Caspase-3 and caspase-9 are particularly important in demonstrating mitochondria-mediated apoptosis [46]. A significant increase in caspase-3 and caspase-9 activity was observed after 24 h of CuONP exposure, indicating the implementation of apoptosis in HEp-2 cells. We further analyzed the mRNA expression of apoptotic genes (p53, bax, bcl2, caspases 3 and 9) in response to CuONP exposure in HEp-2 cells, since the apoptosis is controlled through these pathways. CuONPs increased the mRNA expression of proapoptotic genes p53 and bax, according to the RT-qPCR results. Furthermore, mRNA expression of caspase 3 and 9 genes was found to be increased in CuONP-treated HEp-2 cells. In addition, the antiapoptotic gene, bcl2, was downregulated in HEp-2 cells treated with CuONPs. It is well reported that upregulation of p53 gene leads to activation of proapoptotic members of bcl2 family [47]. Furthermore, bax, a member of the bcl2 family, induced permeabilization of the mitochondrial membrane, allowing soluble proteins to enter the cytosol via the intermembranous space and activate caspases [48]. Similarly, increased levels of caspases 3 and 9 in HEp-2 cells after CuONP exposure indicated execution of mitochondria-mediated apoptosis. CuONPs have previously been shown to cause cell death in other cell types via a mitochondria-mediated pathway [14, 49].

Conclusion

We found that CuONPs induced significant cytotoxicity in HEp-2 cells at low concentrations ranging from 2 to 40 µg/ml in a dose-dependent manner. CuONP-induced oxidative stress further tempted cellular damage which resulted in ROS generation. These findings also support the mitochondrial dysfunction and activation of caspases as a primary target of CuONPs in HEp-2 cells. Moreover, quantitative real-time PCR results demonstrated that mRNA expression of apoptotic marker genes was altered by CuONP exposure. These findings imply that CuONPs can induce apoptosis in HEp-2 cells via the p53, bax, bcl2, and caspase pathways. These molecular changes shed light on the mechanisms by which CuONPs cause cytotoxicity, oxidative stress, ROS production, mitochondrial dysfunction, caspase activation, and apoptotic HEp-2 cell death. Furthermore, the current study calls for additional research using an in vivo system to determine the effects of CuONP exposure on human health.

Acknowledgements The authors are grateful to the Deanship of Scientific Research, King Saud University, for funding through Vice Deanship of Scientific Research Chairs.

Author Contribution Nida N. Farshori and Maqsood A. Siddiqui conceptualized and designed the experiments, and drafted the manuscript. Mai M. Al-Oqail and Ebtesam S. Al-Sheddi helped in experiments and analyzed the data. Shaza M. Al-Massarani revised and edited the manuscript. Maqusood Ahamed and Javed Ahmad performed nanoparticle characterization and real-time PCR experiments. Abdulaziz A. Al-Khedhairy provided resources and supervised the work.

Data availability Data and materials of this study are available on request.

Declarations

Ethics Approval This paper does not contain any studies with human or animals.

Consent to Participate Not applicable.

Consent for Publication The authors approved processing of this manuscript for publication.

Conflict of Interest The authors declare no competing interests.

References

1. Nations S, Long M, Wages M, Maul JD, Theodorakis CW, Cobb GP (2015) Subchronic and chronic developmental effects of copper oxide (CuO) nanoparticles on Xenopus laevis. Chemosphere 135:166–174
2. El Bialy BE, Hamouda RA, Abd Eldaim MA, El Ballal SS, Heikal HS, Khalifa HK, Hozzein WN (2020) Comparative toxicological effects of biologically and chemically synthesized copper oxide nanoparticles on mice. Int J Nanomed 15:3827–3842
3. Siddiqi KS, Husen A (2020) Current status of plant metabolite-based fabrication of copper/copper oxide nanoparticles and their applications: a review. Biomater Res 24:1–5
4. Pendashteh A, Mousavi MF, Rahmanifar MS (2013) Fabrication of anchored copper oxide nanoparticles on graphene oxide nanosheets via an electrostatic coprecipitation and its application as supercapacitor. Electrochim Acta 88:347–357
5. Naseer B, Srivastava G, Qadri OS, Faridi SA, Islam RU, Younis K (2018) Importance and health hazards of nanoparticles used in the food industry. Nanotechnol Rev 7(6):623–641

6. Naz S, Gul A, Zia M (2019) Toxicity of copper oxide nanoparticles: a review study. IET Nanobiotechnol 14(1):1–3
7. Longano D, Ditaranto N, Sabbatini L, Torsi L, Cioffi N (2012) Synthesis and antimicrobial activity of copper nanomaterials. In: Cioffi N, Rai M. (eds) Nano-Antimicrobials. Springer, Berlin, Heidelberg. https://doi.org/10.1007/978-3-642-24428-5_3
8. Aksakal FI, Ciltas A (2019) Impact of copper oxide nanoparticles (CuO NPs) exposure on embryo development and expression of genes related to the innate immune system of zebrafish (Danio rerio). Comp Biochem Phys C Toxicol Pharmacol 223:78–87
9. Chang YN, Zhang M, Xia L, Zhang J, Xing G (2012) The toxic effects and mechanisms of CuO and ZnO nanoparticles. Materials 5(12):2850–2871
10. Che X, Ding R, Li Y, Zhang Z, Gao H, Wang W (2018) Mechanism of long-term toxicity of CuO NPs to microalgae. Nanotoxicology 12(8):923–939
11. Janani B, Al Farraj DA, Raju LL, Elshikh MS, Alkubaisi NA, Thomas AM, Das A, Khan SS (2020) Cytotoxicological evaluation of copper oxide nanoparticles on green algae, bacteria and crustacean systems. J Environ Health Sci Eng 18(2):1465–1472
12. Kasemets K, Ivask A, Dubourguier HC, Kahru A (2009) Toxicity of nanoparticles of ZnO, CuO and TiO_2 to yeast Saccharomyces cerevisiae. Toxicol In Vitro 23(6):1116–1122
13. Ahamed M, Siddiqui MA, Akhtar MJ, Ahmad I, Pant AB, Alhadlaq HA (2010) Genotoxic potential of copper oxide nanoparticles in human lung epithelial cells. Biochem Biophys Res Commun 396(2):578–583
14. Siddiqui MA, Alhadlaq HA, Ahmad J, Al-Khedhairy AA, Musarrat J, Ahamed M (2013) Copper oxide nanoparticles induced mitochondria mediated apoptosis in human hepatocarcinoma cells. PLoS One 8(8):e69534
15. Fu X (2015) Oxidative stress induced by CuO nanoparticles (CuO NPs) to human hepatocarcinoma (HepG2) cells. J Cancer Ther 6(10):889–895
16. Fahmy HM, Ebrahim NM, Gaber MH (2020) *In-vitro* evaluation of copper/copper oxide nanoparticles cytotoxicity and genotoxicity in normal and cancer lung cell lines. J Trace Elem Med Biol 60:126481
17. Sun J, Wang S, Zhao D, Hun FH, Weng L, Liu H (2011) Cytotoxicity, permeability, and inflammation of metal oxide nanoparticles in human cardiac microvascular endothelial cells. Cell Biol Toxicol 27(5):333–342
18. Reddy AR, Lonkala S (2019) *In vitro* evaluation of copper oxide nanoparticle-induced cytotoxicity and oxidative stress using human embryonic kidney cells. Toxicol Ind Health 35(2):159–164
19. Shi Y, Pilozzi AR, Huang X (2020) Exposure of CuO nanoparticles contributes to cellular apoptosis, redox stress, and Alzheimer's Aβ amyloidosis. Int J Environ Res Public Health 17(3):1005
20. Luo C, Li Y, Yang L, Zheng Y, Long J, Jia J, Xiao S, Liu J (2014) Activation of Erk and p53 regulates copper oxide nanoparticle-induced cytotoxicity in keratinocytes and fibroblasts. Int J Nanomedicine 9:4763–4772
21. He H, Zou Z, Wang B, Xu G, Chen C, Qin X, Yu C, Zhang J (2020) Copper oxide nanoparticles induce oxidative DNA damage and cell death via copper ion-mediated p38 MAPK activation in vascular endothelial cells. Int J Nanomedicine 15:3291–3302
22. Bugata LS, Pitta Venkata P, Gundu AR, Mohammed Fazlur R, Reddy UA, Kumar JM, Mekala VR, Bojja S, Mahboob M (2019) Acute and subacute oral toxicity of copper oxide nanoparticles in female albino Wistar rats. J Appl Toxicol 39(5):702–716
23. Wongrakpanich A, Mudunkotuwa IA, Geary SM, Morris AS, Mapuskar KA, Spitz DR, Grassian VH, Salem AK (2016) Size-dependent cytotoxicity of copper oxide nanoparticles in lung epithelial cells. Environ Sci Nano 3(2):365–374
24. Murdock RC, Braydich-Stolle L, Schrand AM, Schlager JJ, Hussain SM (2008) Characterization of nanomaterial dispersion in solution prior to in vitro exposure using dynamic light scattering technique. Toxicol Sci 101(2):239–253
25. Siddiqui MA, Saquib Q, Ahamed M, Farshori NN, Ahmad J, Wahab R, Khan ST, Alhadlaq HA, Musarrat J, Al-Khedhairy AA, Pant AB (2015) Molybdenum nanoparticles-induced cytotoxicity, oxidative stress, G2/M arrest, and DNA damage in mouse skin fibroblast cells (L929). Colloids Surf B Biointerfaces 125:73–81
26. Siddiqui MA, Kashyap MP, Kumar V, Al-Khedhairy AA, Musarrat J, Pant AB (2010) Protective potential of trans-resveratrol against 4-hydroxynonenal induced damage in PC12 cells. Toxicol In Vitro 24(6):1592–1598
27. Buege JA, Aust SD (1978) Microsomal lipid peroxidation. Methods Enzymol 52:302–310
28. Chandra D, Ramana KV, Wang L, Christensen BN, Bhatnagar A, Srivastava SK (2002) Inhibition of fiber cell globulization and hyperglycemia-induced lens opacification by aminopeptidase inhibitor bestatin. Invest Ophthalmol Vis Sci 43(7):2285–2292
29. Farshori NN, Saquib Q, Siddiqui MA, Al-Oqail MM, Al-Sheddi ES, Al-Massarani SM, Al-Khedhairy AA (2021) Protective effects of *Nigella sativa* extract against H_2O_2-induced cell death through the inhibition of DNA damage and cell cycle arrest in human umbilical vein endothelial cells (HUVECs). J Appl Toxicol 41(5):820–831
30. Al-Oqail MM, Al-Sheddi ES, Farshori NN, Al-Massarani SM, Al-Turki EA, Ahmad J, Al-Khedhairy AA, Siddiqui MA (2019) Corn silk (*Zea mays* L.) induced apoptosis in human breast cancer (MCF-7) cells via the ROS-mediated mitochondrial pathway. Oxid Med Cell Longev 2019: 9789241
31. Al-Oqail MM, Al-Sheddi ES, Al-Massarani SM, Siddiqui MA, Ahmad J, Musarrat J, Al-Khedhairy AA, Farshori NN (2017) *Nigella sativa* seed oil suppresses cell proliferation and induces ROS dependent mitochondrial apoptosis through p53 pathway in hepatocellular carcinoma cells. South Afr J Bot 112:70–78
32. Ahmad J, Wahab R, Siddiqui MA, Saquib Q, Ahmad N (2021) Al-Khedhairy AA (2021) Strontium-doped nickel oxide nanoparticles: synthesis, characterization, and cytotoxicity study in human lung cancer A549 cells. Biol Trace Elem Res. https://doi.org/10.1007/s12011-021-02780-5
33. Patterson AL (1939) The Scherrer formula for X-ray particle size determination. Phys Rev 56(10):978–982
34. Morsy EA, Hussien AM, Ibrahim MA, Farroh KY, Hassanen EI (2021) Cytotoxicity and genotoxicity of copper oxide nanoparticles in chickens. Biol Trace Elem Res 199:4731–4745
35. Akhtar MJ, Kumar S, Alhadlaq HA, Alrokayan SA, Abu-Salah KM, Ahamed M (2016) Dose-dependent genotoxicity of copper oxide nanoparticles stimulated by reactive oxygen species in human lung epithelial cells. Toxicol Ind Health 32(5):809–821
36. Liu H, Lai W, Liu X, Yang H, Fang Y, Tian L, Li K, Nie H, Zhang W, Shi Y, Bian L (2021) Exposure to copper oxide nanoparticles triggers oxidative stress and endoplasmic reticulum (ER)-stress induced toxicology and apoptosis in male rat liver and BRL-3A cell. J Hazard Mater 401:123349
37. Assadian E, Zarei MH, Gilani AG, Farshin M, Degampanah H, Pourahmad J (2018) Toxicity of copper oxide (CuO) nanoparticles on human blood lymphocytes. Biol Trace Elem Res 184(2):350–357
38. Yu Z, Li Q, Wang J, Yu Y, Wang Y, Zhou Q (2020) Li P (2020) Reactive oxygen species-related nanoparticle toxicity in the biomedical field. Nanoscale Res Lett 15:115. https://doi.org/10.1186/s11671-020-03344-7
39. Sena LA, Chandel NS (2012) Physiological roles of mitochondrial reactive oxygen species. Mol Cell 48(2):158–167
40. Kung ML, Hsieh SL, Wu CC, Chu TH, Lin YC, Yeh BW, Hsieh S (2015) Enhanced reactive oxygen species overexpression by CuO nanoparticles in poorly differentiated hepatocellular carcinoma cells. Nanoscale 7(5):1820–1829

41. Gaetke LM, Chow CK (2003) Copper toxicity, oxidative stress, and antioxidant nutrients. Toxicology 189(1–2):147–163
42. Oladimeji O, Akinyelu J, Singh M (2020) Co-polymer functionalised gold nanoparticles show efficient mitochondrial targeted drug delivery in cervical carcinoma cells. J Biomed Nanotechnol 16(6):853–866
43. Reed JC, Kroemer G (2000) Mechanisms of mitochondrial membrane permeabilization. Cell Death Differ 7(12):1145
44. Jouan E, Le Vee M, Denizot C, Da Violante G, Fardel O (2014) The mitochondrial fluorescent dye rhodamine 123 is a high-affinity substrate for organic cation transporters (OCT s) 1 and 2. Fundam Clin Pharmacol 28(1):65–77
45. Mahalakshmi M, Kumar P (2019) Phloroglucinol-conjugated gold nanoparticles targeting mitochondrial membrane potential of human cervical (HeLa) cancer cell lines. Spectrochim Acta A Mol Biomol Spectrosc 219:450–456
46. Li J, Yuan J (2008) Caspases in apoptosis and beyond. Oncogene 27(48):6194–6206
47. Pietsch EC, Sykes SM, McMahon SB, Murphy ME (2008) The p53 family and programmed cell death. Oncogene 27(50):6507–6521
48. Dadsena S, Jenner A, García-Sáez AJ (2021) Mitochondrial outer membrane permeabilization at the single molecule level. Cell Mol Life Sci 78(8):3777–3790
49. Shafagh M, Rahmani F, Delirezh N (2015) CuO nanoparticles induce cytotoxicity and apoptosis in human K562 cancer cell line via mitochondrial pathway, through reactive oxygen species and P53. Iran J Basic Med Sci 18(10):993–1000